Article

Special-Oriented Annealing Twins Induced Orange Peel Morphology of Heat Pipe under Bending Deformation

Song-Wei Wang *, Hong-Wu Song, Shi-Hong Zhang and Shuai-Feng Chen

Shi-changxu Innovation Center for Advanced Materials, Institute of Metal Research, Chinese Academy of Sciences, Shenyang 110016, China; swwang16b@imr.ac.cn (S.W. W.); hwsong@imr.ac.cn (H.W. S.); shzhang@imr.ac.cn (S.H. Z.); chensf@imr.ac.cn (S.F. C.)

* Correspondence: swwang16b@imr.ac.cn (Y. X.) TEL.: +86-024-8397 0203

Abstract: Thin-wall heat pipe is an efficient heat transfer component, which has been widely used in the field of heat dissipation of high-power electronic equipment in recent years. In this study, the orange peel morphology defect of thin-wall heat pipes after bending deformation was analyzed both for the macro 3D profile and for the micro-formation mechanism. The morphology and crystal orientations of the grains and annealing twins were carefully characterized utilizing optical metallography and electron backscatter diffraction technique. The results show that after high-temperature sintering treatment, the matrix grains of the heat pipe are coarsened seriously and formed a strong Goss texture, while certain annealing twins with the unique Copper orientation are retained. The distribution of the Schmid factor value subjected to the uniaxial stress indicate the inhomogeneity of intergranular deformation exists among the annealing twins and matrix grains. The annealing twin exhibit a "hard-oriented" component during the deformation; thus, it plays a role as a barrier and hinders the slipping of dislocation. As the strain accumulates, part of the annealing twins may protrude from the surface of the heat pipe, forming a large-scale fluctuation of the surface as the so-called "orange peel" morphology. The 3D profile shows the bulged twins mostly perpendicular to the drawing direction, with about 200-300μm in width and 10-20μm in height.

Keywords: surface roughening; heat pipe; annealing twin; texture

1. Introduction

The heat pipe is widely used in the field of electronic appliances (such as computers, fans, and cell-phone, et al) due to its high efficiency of heat conduction. However, the surface roughening problem, so-called "orange peel", after bending deformation of the heat pipe is raised as a limitation for its application. Orange peel defects as a surface roughening phenomenon have drawn great attention due to their negative effects on forming process and product quality, which was generally noticed in science and industry [1]. This type of surface defect will bring the bad aspects as follows: (1) affects the beauty of the product, which makes it difficult to be used in the field of high-end equipment heat dissipation; (2) decrease the heat transfer efficiency by affecting the fitting degree of the outer surface of the heat pipe and the connecting surface, which is easy to produce voids, thus affecting the heat transfer; (3) decline of surface quality after bending deformation. Thus, the specification and control of the unwilling surface topography is an essential manufacturing requirement. Therefore, figuring out the influencing factors are of great importance for research purposes and manufacturing control.

Surface roughening problems for FCC metals, i.e., aluminum alloys and steels have been studied massively both by experimental and numerical methods. The influence of the microstructure aspect (such as grain size and texture) and the loading condition (such as temperature and strain rate) on the orange peel, ridging, and roping has been researched. Many results have confirmed that the surface roughening is strongly dependent on the grain size of materials during deformation [2-5]. Dai investigated the plastic deformation-induced surface roughening mechanism of aluminum sheets. The average grain

 doi:10.20944/preprints202302.0334.v1

rotation and grain size are found to be the dominant contributor to the surface vertical characteristics such as the root-mean-square roughness. The surface horizontal characteristic such as the correlation length is found to be mainly determined by the average grain size. Also, studies on the relationship between plastic strain and deformation-induced roughness were carried out [6-9]. Cai et al. [9] present an interesting approach to obtaining the continuous strain distribution on a sample after deformation. By using a specially designed stage, it was possible to measure changes in surface roughness in situ for increasing tensile load. The results showed that the surface roughness increased when the strain was below a certain value, and slightly decreased as the strain increased. Recently, the investigations [10-15] have been focusing on understanding the formation mechanism of surface roughness. Utilizing the electron backscatter diffraction (EBSD) technique, the crystallographic orientation of grains on the surface can be characterized. And this information can be directly incorporated into the finite element method (FEM) by simulation software. Kishimoto et al. [12] considered that the crystal orientation, suppresses the development of the inner surface roughness of the micro-tube, which can be investigated by evaluating the crystal orientation of the inner surface when increasing and decreasing wall thickness during the new hollow sinking process. The results reported that the outer surface roughness developed during the new hollow sinking because of the excessive thinning of the outer diameter. Wu et al. [13] developed a 3D crystal plasticity finite-element model to simulate the development of a rope-like surface roughness profile, and the results demonstrated that the 3D spatial distribution of specific grain orientations is the determinant factor for surface roughening. Similar results were observed by Wilson [14]during hydro-forming and bending deformation, respectively. Romanova et al. [15] proposed a three-dimensional model of the material with a hardened layer of varying thickness and strength compared to the initial material. A numerical analysis was carried out by the finite difference methods. It was found that internal stresses appearing at the layer boundary and bulk material are responsible for surface roughness which gets larger as the hardened layer gets thinner. It was observed that the local increase in irregularities is due to the movement of connected grains.

Although there have been many studies on the surface roughening problem represented by the defect of orange peel, its formation mechanism is still worth discussing due to the complexity of the deformation materials and heat treatment process. The thin-walled heat pipes discussed in this paper have unique sintering process and structure characteristics. After the high-temperature heat treatment, the grains grow up serious though the recrystallization and growth stage, and especially, a lot of annealing twins are generated in pure copper. The effects of grain size and annealing twins on the surface roughening need to be investigated which is still in lack of reports. In practical applications, these heat pipes have usually been bent into various shapes as required, thus the orange peel morphology on the outer surface needs to be solved to improve the quality of heat pipe products. It is meaningful to better understand the formation mechanism of the surface defect and to provide a reference for production.

2 Materials and Methods

The material used for heat pipes is pure copper with a composition of 99.996%. The size of heat pipes is Φ6×0.3 mm, and the thickness-diameter ratio reaches 0.05. The heat pipe was manufactured by a complex procedure. The initial pipe was prepared by multi-passes of float-plug drawing (FPD) process followed by an annealing treatment. To get a semi-hardening state, one more FPD process was imposed on the pipe with a 30-35% area reduction. And the heat pipes billet was obtained with the size ofΦ6×0.3 mm. Then 980℃ ×3.5 h sintering treatment was carried out at the vacuum furnace after copper powder was filled into the billet. Finally, the pipes were filled with special liquids and sealed to make an internal vacuum, and then the heat pipes were finished. To simulate the rotary bending performance in this experiment, the bending radius was chosen R=10.5mm and the bending angle was 180 degrees.

Preprints (www.preprints.org) | NOT PEER-REVIEWED | Posted: 20 February 2023 doi:10.20944/preprints202302.0334.v1

The microstructure of the pipe wall after bending deformation was observed by optical microscope (OM) at the view section A and B, the location where the samples took from can be seen in Fig. 1. The scanning electron microscopy (SEM) analysis was carried out by FEI Nova Nano scanning electron microscope equipment to observe the whole macrostructure of "orange peel" morphology. The observation area was selected at the maximum bent part as marked by the black dotted box in Fig. 1. The samples were cleaned by the ultrasonic wave in an alcohol solution and then observed directly without the grinding process. By using this method, the original state of the surface roughness will be preserved. To investigate the local 3D profile of the bulge of the bent surface, a Micro XAM surface mapping microscope was used to measure the surface properties. Since the whole bent area is too large to measure as well as the bent surface lead to different distance to the lens, the local section on the bent area was chosen to observe. The scan area is a square with a side length of 728μm and the scan step is 1.45nm. The crystallographic orientations of the "orange peel" section were measured with electron backscatter diffraction (EBSD) on the FEI Nova Nano SEM 430 field-emission scanning electron microscope equipped with fully automatic HKL technology. The EBSD samples for EBSD measurements were cut from a bending surface (seen in Fig. 1) with 5mm in length (DD), 3mm in width (CD), and from the surface of sintered pipes with 5mm in length (DD), 2mm in width (CD). The samples were slightly ground and then polished, followed by an electropolishing treatment. The local coordinate system of the EBSD sample was defined as seen in Fig. 1, and the DD-CD section was set as the observation plane. The EBSD maps were acquired using a step size of 6μm to analyze the grains and annealing twins. The indexing rate was 100%. In this study, a critical misorientation angle of 2° was applied to observe boundaries in the orientation maps, where low-angle grain boundaries (LAGBs) and high-angle grain boundaries (HAGBs) were defined as boundaries between grains with misorientation 2-10° and >10°, respectively.

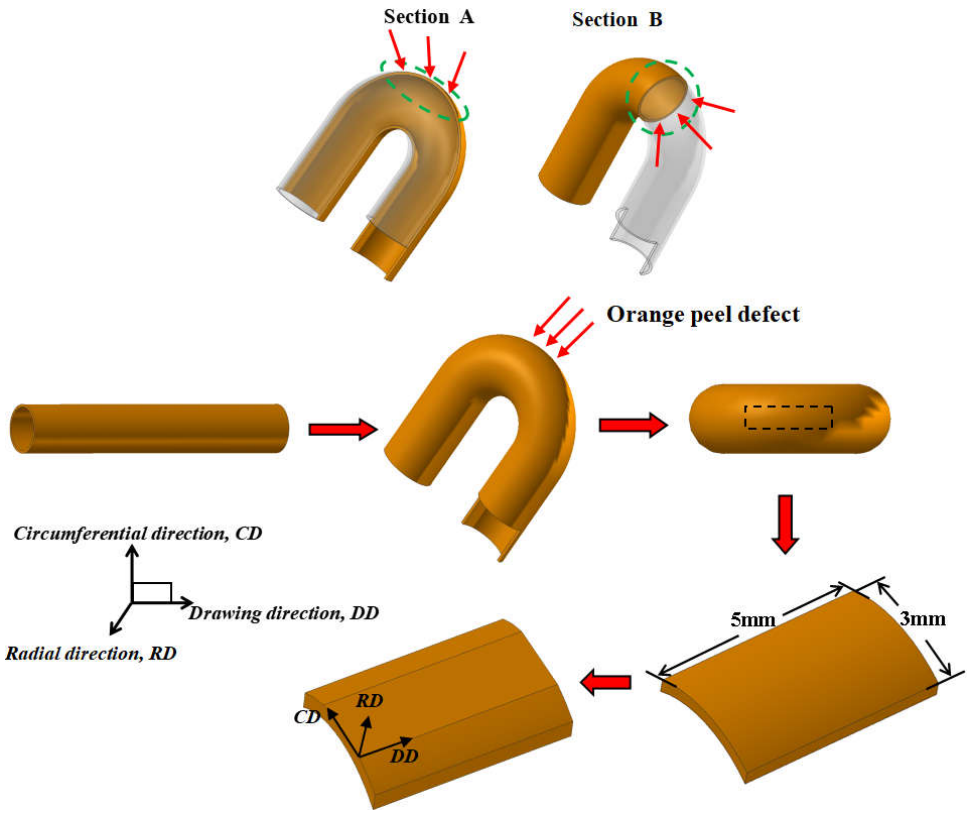

Figure 1. The selection and location of samples on the bent heat pipe.

Preprints (www.preprints.org) | NOT PEER-REVIEWED | Posted: 20 February 2023 doi:10.20944/preprints202302.0334.v1

3 Results and Discussion

3.1. Microstructure of the heat pipe after bending deformation

The heat pipe underwent high-temperature sintering treatment of 980℃×3.5 h, resulting in full recrystallization and severe grain growth. The microstructure of the heat pipe at the bent area along the longitudinal slice and transverse slice marked as section A and section B (Fig. 1), respectively, have been examined using an optical microscope (OM) as seen in Fig. 2. To provide a comprehensive view of the pipe microstructure, multiple images were combined and stitched together. It is clear to observe the annealing twins of band-shape present in the matrix grains. The FCC metals of low to medium stacking fault energy tend to have a preponderance of forming annealing boundaries in the recrystallization process [16-18]. The pure copper with medium stacking fault also prefers to form the annealing twins during recrystallization, and the details were reported by Field [19]. The annealing twins show the difference in brightness after etching due to its unique orientation relationship with the matrix, as seen in Fig. 2a, b marked in a white dotted circle. The distinct grain boundaries were highlighted in the green circles in Fig. 2a, making it easy to identify that only one layer of grain was present in the pipe wall. The porous structure formed by copper powder sintering can be seen on the inner side of the pipe wall, which provides certain support to the inner side of the bending and prevents wrinkling. It can be concluded that the grains coarsen severely during the sintering treatment. These annealing twins grow with the matrix grains and become broader in width and reach the whole wall thickness in length. At the bent section, the annealing twins bulge out the outer side surface of the heat pipe. Fig. 2b shows the enlarged schematic diagram of the bulged annealing twin, the Δd is the value of the distance of the bulge. The protruding height Δd of the bent area to the surface is approximately 10-20μm, which contributes to the "orange peel" morphology.

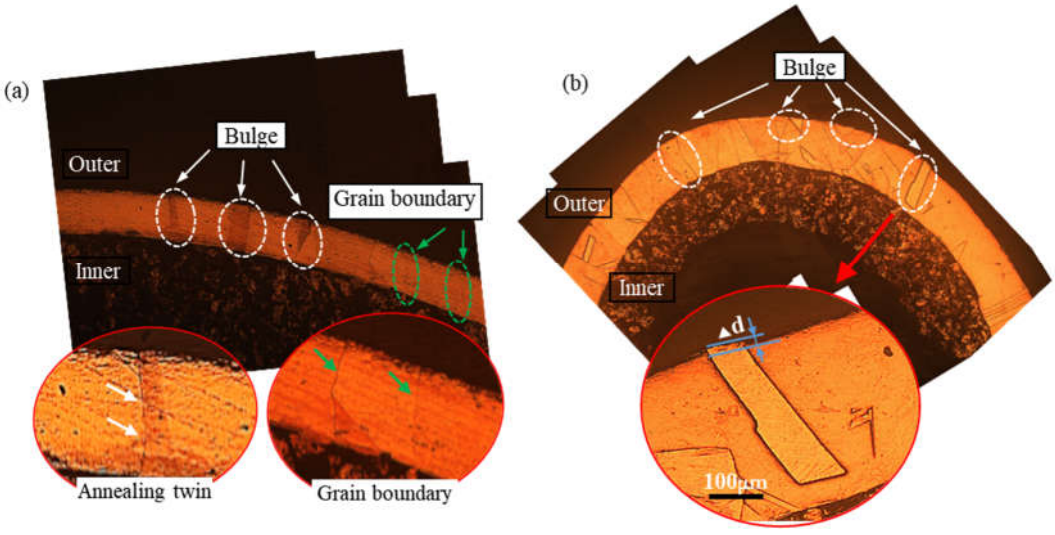

Figure 2. The microstructure of the outside of the bent pipe along longitudinal slice (a) section A and transverse slice (b) section B and the enlarged schematic diagram of the pipe wall bulge.

3.2 Characterization of "orange peel" morphology on the bent surface

Fig. 3 shows the outer surface at the maximum bending position of the "orange peel" pipe and the normal pipe as a comparison. It is easy to see the orange peel defect by visual inspection as it presents an uneven surface and a gloomy look (Fig. 3a), while the normal pipe shows a smooth surface (Fig. 3c). The uneven surface will strongly affect the quality of the heat pipe product. A backscatter electron image (BSE) was used to examine the micro-surface topography of the bent zone marked by the black box in Fig. 3a, and c, respectively. The bent section observed at a magnification of 50× shows an uneven surface result from the band-like bulge as marked by white arrows. While the bent section on the

Preprints (www.preprints.org) | NOT PEER-REVIEWED | Posted: 20 February 2023 doi:10.20944/preprints202302.0334.v1

normal pipe shows the slip bands (marked by yellow arrows) produced during the bending deformation that is about 45 degrees to the longitudinal direction. The remained slip band on the surface indicated the good plasticity of the normal pipe, and the direction of the slip bands revealed the mainly tensile stress along the longitudinal direction. The results confirm the conclusion obtained by research of Romanova [4], the smallest out-of-plane surface displacements are attributed to intra-grain dislocation glide, and the larger displacements are associated with small grains movement and give rise to the formation of the orange peel pattern. In the copper pipes after sintering treatment the annealing twins grow up with the recrystallized grains. During the bending process, the outer side surface of the pipe was mainly subjected to tensile stress. These annealing twins cannot coordinate with the matrix grains during deformation and interrupted the slipping of dislocation and hindered plastic deformation.

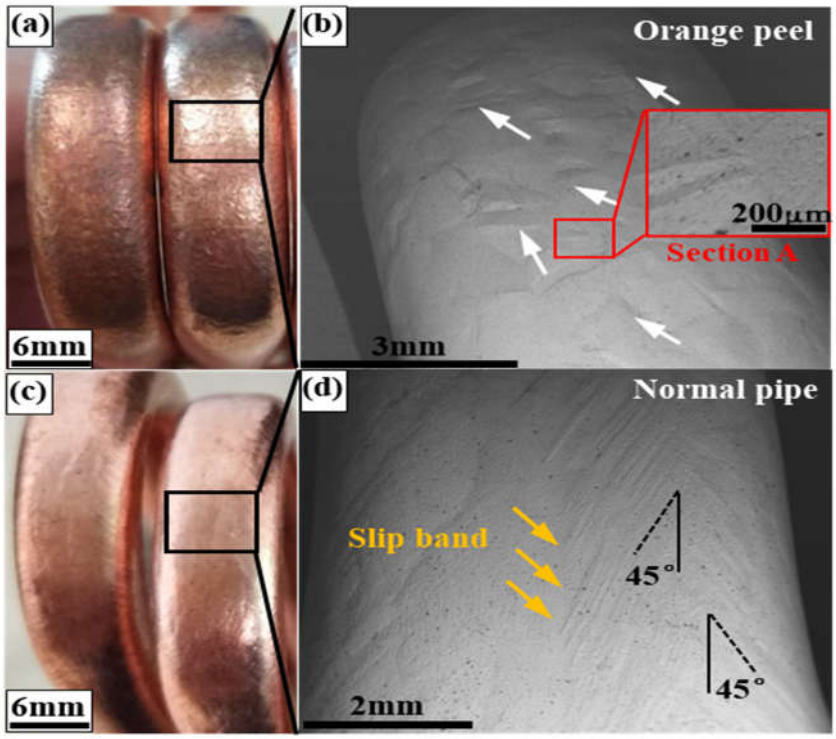

Figure 3. Orange peel morphology on the bending section of the heat pipe (a) (b) and the compared no-peel pipe (c) (d) by visual inspection (a) (c) and by SEM observation (b) (d).

In order to investigate the 3D profile of the bulge on the surface, the surface mapping microscope was used to examine a certain section A (Fig. 3b) with a size of 728μm×728μm. Fig. 4a shows the "hill and valley" morphology due to the fluctuation at height (Z-axis direction) which is indicated by variable color legend in Fig. 4c. There is a gradual decrease in height at the edge because of the curved surface, but it does not affect the observation of bulge area. It can be observed that the band-like annealing twins protrude from a surface with clear grain boundaries, which is in corresponds to the results measured in Fig. 2b. Fig. 4c showed the height undulations along with the dotted line AB in the middle of the region. The peak values of the curve in Fig. 4c appear at the positions corresponding to the annealing twins. The bulged twins are mostly perpendicular to the DD, and with about 200-300μm in width and about 10μm in height. The micro-characteristic feature of valleys and hills forms the "orange peel" defects on the bent surface of the heat pipe.

Preprints (www.preprints.org) | NOT PEER-REVIEWED | Posted: 20 February 2023 doi:10.20944/preprints202302.0334.v1

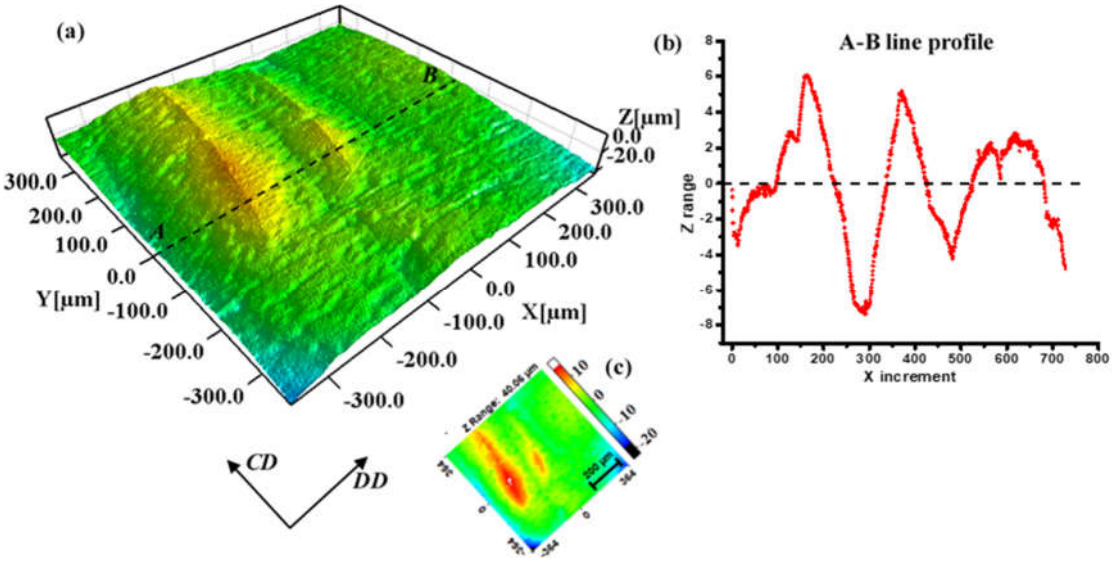

Figure 4. 3D profile of the bulged grains on the orange peel surface:(a) false color topography image; (b) distribution of Z range along line AB; (c) legend of the 3D profile.

Electron backscatter diffraction (EBSD) observations were carried out to further examine the grain orientations of the bent surface. The sample was taken from the bent section as shown in Fig.3a and the DD-CD plane was taken as the observation plane for EBSD measurement. Fig.5a illustrates the grain orientations of the orange peel surface, the annealing twins colored purple (marked by black arrows) show an obvious difference orientation with the matrix grains of green color. These specially oriented "band-like" annealing twins exhibit a sharply discordant orientation with the matrix grains. Fig. 5b shows the distribution of misorientation angle that the curve presents two peaks, which is in corresponding to the low angle grain boundaries (LABs) and the twin-relationship (Σ3) boundaries, respectively. During the grains coarsen process, the matrix grains encounter each other and form LABs, as seen in Fig. 5a. The texture components were analyzed by pole figure based on the EBSD information, as seen in Fig. 5c. [20]. The observation plane was defined by the DD-CD surface (the normal direction is RD) at the EBSD measurement. As a result, we can determine the relationship between the sample coordinate system and the crystal coordinate system as follows: for example, the Goss texture component means that the {110} crystal plane parallel to the observation plane (DD-CD plane), and the <001> crystal direction parallel to the DD direction.

Preprints (www.preprints.org) | NOT PEER-REVIEWED | Posted: 20 February 2023 doi:10.20944/preprints202302.0334.v1

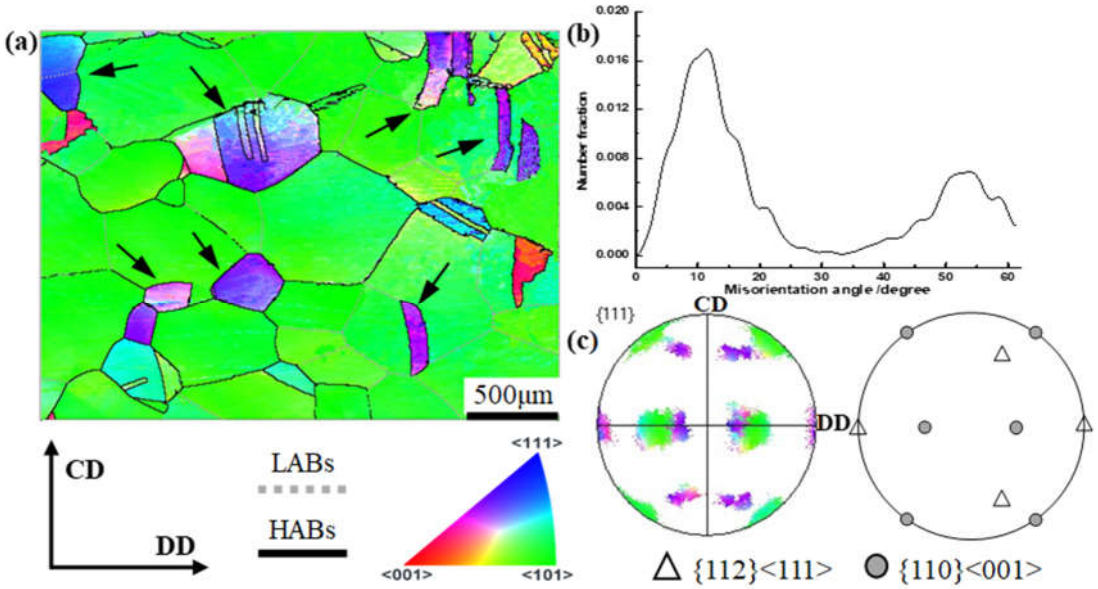

Figure 5. EBSD maps, pole figure, and misorientation distribution of the bent surface of the peel pipe: (a) IPF; (b) misorientation angle distribution; (c) pole figure.

3.3 Deformation inhomogeneity between annealing twins and matrix grains

The above results indicate that these bulge regions on the surface originate from the annealing twins. Therefore, the sample of peel pipe before bending deformation was prepared for EBSD characterization as seen in Fig. 6a. The observation plane was also on the DD-CD surface. The black lines represent high-angle grain boundaries (with a misorientation angle >10°). From the IPF map, it is obvious that the matrix grains in green color grew up severely and combined finally, in order to see clearly, the low angle grain boundaries were removed. In addition, the texture components are similar to the bent tube, that is, the Goss component of green grains is the main texture, accompanied by an amount of Copper texture composed of the annealing twins. Compared with the bent tube, the color of the twins of Copper texture in the pre-bent tube is somewhat different, which is due to the orientation deviations. In this paper, the allowable deviation range for texture calculation is within 10 ° from the ideal texture orientation. The orientations of the crystal may change a bit due to the bent process, but can not change the texture type with such a small deformation. It is confirmed that the matrix and the annealing twins form the Goss and Copper textures respectively as a result of the sintering treatment. Thus, the annealing twins in purple/pink color contribute to the discordant orientation with the matrix grains, i.e., the "special orientation". It is noticed that another annealing twin variant in green orientation exists in the matrix grains, which is disappeared after bending deformation. The 3D crystal cubic of orientation components was illustrated in Fig. 6a. The relationships between the two types of annealing twins (define as T1 and T2) are calculated at about 59.9 ° <111> and 55.9 ° <111>, respectively. The annealing twin variants are nucleated on the {111} crystal plane as a growing accident because of the low stacking faults.

It is known that slip is the main deformation style of pure copper with 5 independent {111} <110> slip systems. With the grain-orientations information obtained from EBSD, it is possible to measure the activity of the slip system by the Schmid factor (SF). In this study, the SF calculation is important to understanding the intergranular scale deformation behavior. It is known that the SF value is dependent on the direction of applied stress and the deformation mode of certain grain orientations. The loading condition of the pipe during the rotary bending process is complex because of the stress and strain gradients that exist in the pipe. The analysis of stress distribution has been researched both by theoretical calculation and by finite element simulation methods [21-23]. However, it is difficult to measure an accurate stress state during the bending process because macroscopic stress is not a constant. Moreover, the local stresses among individual grains

 doi:10.20944/preprints202302.0334.v1

are also various. From the previous results, the stress tensor can be reduced to a set of principal stresses: major stress along DD (σ_1), stress along CD (σ_2), and the stress along the normal direction (σ_3) of the observation plane (DD-CD). The σ_1 is assumed as the main stress leading to the tensile strain of the extrados surface, i.e., the $\sigma_1 >> \sigma_2$ and σ_3, that equivalent to the uniaxial stress for SF value calculations. The SF value does not have strict physical meaning, but it is helpful to evaluate, on a comparative basis, the deformation resistance as well as the deformation uniformity in this study [24].

Fig. 6b shows the SF distribution of peel pipe before bending deformation. The value of SF is equal in the individual matrix grain, except for the part divided by the annealing twins. From the result of the Schmidt factor calculation, there are three peaks in the curve. Compared with Fig. 6a, the highest peak corresponds to the matrix grains, with the maximum Schmidt factor value is about 0.43. The next two small peaks with the value of about 0.36 and 0.28 are corresponding to the pink color annealing twins and the purple color and part of green color annealing twins, respectively. The SF value of the annealing twins is lower than the matrix grains on average. The SF fraction curve with several peaks shows the inhomogeneous deformation behavior among the grains. It is known that the SF is used to evaluate the activation of deformation modes, i.e., with the highest SF, the slip system has the greatest possibility to be activated. The existence of annealing twins in the matrix decreases the uniformity of the distribution of SF, that is to say, it decreases the uniformity of the deformation of grains. Moreover, the slip propagation across the grain boundary is primarily connected with the neighboring grains' orientation (the type of grain boundary) and their relation with respect to the direction of operating forces. It has been confirmed that dislocation transmission through the twin-type boundaries is never a direct transfer [25]. Dislocation pile-ups or decomposition in the boundary occurs, which makes the twins act as an effective barrier to slip [26].

From above, it is concluded that the inhomogeneity of the deformation is created by the presence of annealing twins from the pre-bent condition and then they further influence the deformation during bending. After the sintering process, the matrix grains seriously coarsen and merge into together. While the annealing twin with the unique twin-type boundary relationship may act as a hinder to the slipping of dislocation, which leads to the deformation inhomogeneously in grains, as seen in Fig. 7. The inhomogeneous intergranular deformation caused the uneven surface of the bent tube, the so-called of "orange peel" morphology.

Preprints (www.preprints.org) | NOT PEER-REVIEWED | Posted: 20 February 2023 doi:10.20944/preprints202302.0334.v1

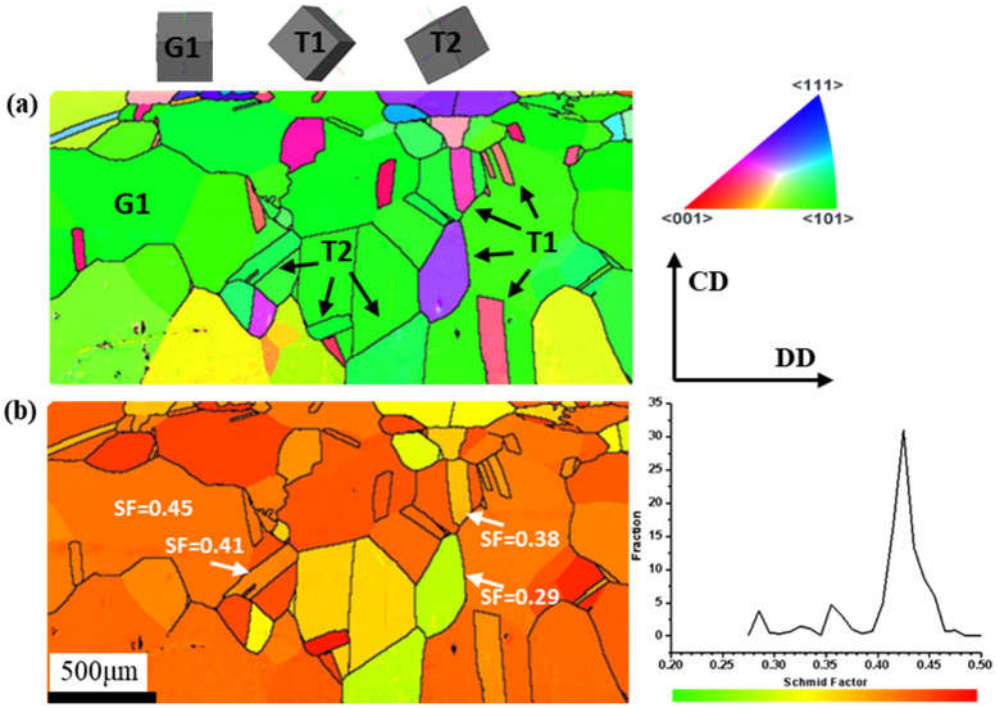

Figure 6. EBSD maps and Schmid factor distribution of peel pipe before bending deformation: (a) IPF; (b) Schmid factor distribution.

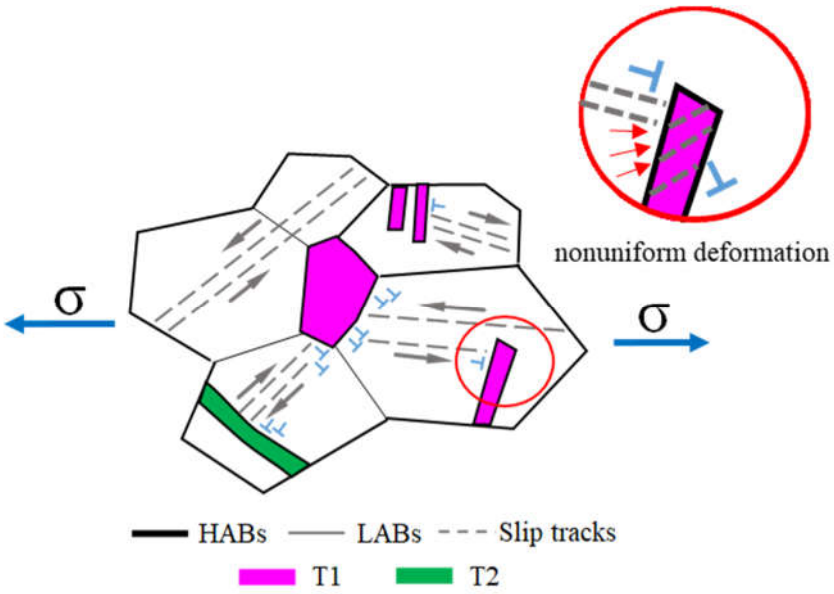

Figure 7. Schematic diagram of the intergranular nonuniform deformation subjected to the uniaxial stress state.

5. Conclusions

In this work, the micro and macro-structure and forming mechanism of orange peel defect on the bent surface of heat pipe were studied. The main conclusions can be summarized as follows:

(1) The "orange peel" defect of the heat pipe is caused by the inhomogeneous intergranular deformation between the annealing twins and the matrix grains, which exhibit the nonuniform in size and crystal orientation. The annealing twins exhibit a hard orientation in bending deformation and may bulge out on the pipe surface, which presents an uneven morphology.

(2) The matrix grains coarsen seriously and form a strong {110} <001> Goss texture during the high-temperature sintering treatment, while the annealing twins in it show a {112} <111> Copper texture. Thus, the annealing twins in it act as a barrier for the slip of dislocations both by the unique orientation with the matrix grains and by the twin-type boundaries.

(3) According to the above results, it is suggested that the orange peel defect on the bending surface of the heat pipe can be relieved by reducing or eliminating the proportion of "hard oriented" annealing twins, or by inhibiting the recrystallized grains growth, such as adding alloying elements.

Author Contributions: "Conceptualization, S.W. W. (Song-Wei Wang) and S.H. Z. (Shi-Hong Zhang); methodology, S.W. W. (Song-Wei Wang) and H.W. S. (Hong-Wu Song); validation, S.W. W. (Song-Wei Wang); investigation, S.W. W. (Song-Wei Wang); writing—original draft preparation, S.W. W. (Song-Wei Wang); writing—review and editing, S.W. W. (Song-Wei Wang) and S. F. C. (Shuai-Feng Chen); supervision, S.H. Z. (Shi-Hong Zhang), and H.W. S. (Hong-Wu Song); funding acquisition, S.H. Z. (Shi-Hong Zhang).

Funding: This research was supported from "the Key Research Program of the Chinese Academy of Sciences, Grant No. ZDRW-CN-2021-3".

Acknowledgments: The authors would like to express their appreciation to the support by the Key Research Program of the Chinese Academy of Sciences, Grant No. ZDRW-CN-2021-3; and the Guangdong Long-feng Precise Tube Co., Ltd. for supplying experimental materials in the present study.

Conflicts of Interest: The authors declare no conflict of interest.

References

1. Vasiliev, L.L. Heat pipes in modern heat exchangers. Appl. Therm. Eng., 2005, 25, 1-19.
2. Nie, N.; Su, L.H.; Deng, G.Y.; Li, H.J.; Yu, H.L.; Tieu, A.K. A review on plastic deformation induced surface/interface roughening of sheet metallic materials. J. Mater. Res. Tec., 2021, 15, 6574-6607.
3. Miranda, M.L.; Somkuti, P.; Bianchi, D.; Cihak-Bayr, U.; Bader, D.; Jech, M.; Vernes, A. Characterization of orange peel on highly polished steel surfaces. Surf. Eng., 2015, 31, 519-525.
4. Romanova, V.; Balokhonov, R.; Panin, A.; Kazachenok, M.; Kozelskaya, A. Micro-and mesomechanical aspects of deformation-induced surface roughening in polycrystalline titanium. Mater. Sci. Eng. A., 2017, 697, 248-258.
5. Sunal, A.P.; Yasin, K.K.; Onur, K. On the utilization of Sachs model in modeling deformation of surface grains for micro/meso scale deformation processes. J. Manuf. Process, 2021, 68, 1086-1099.
6. Grzegorz, S.; Ryszard, B.; Bartlomiej Z. Deformation-induced roughening by contact compression in the presence of oils with diferent viscosity: experiment and numerical simulation. Tribol. Lett, 2020, 68, 117.
7. Cai, Y.; Wang, X.S.; Du, Y. Surface roughening behavior of the 6063-T4 aluminum alloy during quasi-in situ uniaxial stretching. Materials, 2022, 15, 6265.
8. Liewald, M.; Hönle, S.; Sindel, M. Surface roughening of an aluminum 6016 alloy during bending and hemming. Int. J. Mater. Form., 2015, 9, 1-11.
9. Cai, Y.; Wang, X.S.; Yuan, S.J. Analysis of surface roughening behavior of 6063 aluminum alloy by tensile testing of a trapezoidal uniaxial specimen. Mater. Sci. Eng. A., 2016, 672, 184-193.
10. Guilhem, Y.; Basseville, S.; Curtit, F.; Stéphan, J.M.; Cailletaud, G. Numerical investigations of the free surface effect in three-dimensional polycrystalline aggregates. Comput. Mater. Sci., 2013, 70, 150-162.
11. Rossiter, J.; Brahme, A.; Inal, K.; Mishra, R. Numerical analyses of surface roughness during bending of FCC single crystals and polycrystals. Int. J. Plast., 2013, 46, 82-93.
12. Kishimoto, T.; Sakaguchi, H.; Suematsu, S.; Tashima, K.; Kajino, S.; Gondo, S.; Shinsuke, S. Deformation behavior causing excessive thinning of outer diameter of micro metal tubes in hollow sinking. Metals, 2020, 10, 1315.
13. Shi, Y.; Wu, P.D.; Lloyd, D.J.; Embury, D. Numerical study of surface roughening in blow-formed aluminum bottle with crystal plasticity. Mater. Sci. Eng. A., 2015, 638, 97-105.
14. Shi, Y.; Jin, H.; Wu, P.D.; Lloyd, D.J.; Embury, D. Failure analysis of fusion clad alloy system AA3003/AA6xxx sheet under bending. Mater. Sci. Eng. A., 2014, 610, 263-272.
15. Romanova, V.; Balokhonov, R.; Zinovieva, O. A micro-mechanical analysis of deformation-induced surface roughening in surface-modified polycrystalline materials. Meccanica, 2016, 51, 359-370.
16. Randle, V. Twinning-related grain boundary engineering. Acta. Mater., 2004, 52, 4067-4081.
17. Fullman, R.L.; Fisher, J.C. Formation of annealing twins during grain growth. J. Appl. Phys., 1951, 22, 1350-1355.
18. Field, D.P.; Bradford, L.T.; Nowell, M.M.; Lillo, T.M. The role of annealing twins during recrystallization of Cu. Acta. Mater., 2007, 55, 4233-4241.

19. Hu, H. Texture of metals. Texture, 1974, 1, 233-258.
20. Daxin, E.; Liu, Y.F.; Feng, H.B. Deformation analysis for the rotary draw bending process of circular tubes: stress distribution and wall thinning. Steel. Res. Int., 2010, 81, 1084-1088.
21. Li, H.; Yang, H.; Zhang, Z.Y.; Li, G.J.; Liu, N.; Welo, T. Multiple instability-constrained tube bending limits. J. Mater. Process. Tech., 2014, 214, 445-455.
22. Mentella, A.; Strano, M. Rotary draw bending of small diameter copper tubes: predicting the quality of the cross-section. Proc. IMechE., Part B: J. Engineering Manufacture, 2011, 226, 267-278.
23. Jin, L.; Dong, J.; Sun, J.; Luo, A.A. In-situ investigation on the microstructure evolution and plasticity of two magnesium alloys during three-point bending. Int. J. Plast., 2015, 72, 218-232.
24. Pestman, B.J.; De Hosson, J.Th.M.; Vitek, V.; Schapink, F.W. Interaction between lattice dislocations and grain boundaries in FCC and ordered compounds: A computer simulation. Philos. Mag. A., 1991, 64, 951-969.
25. Randle, V. Mechanism of twinning-induced grain boundary engineering in low stacking-fault energy materials. Acta. Mater., 1999, 47, 4187-4196.